Molecular Cell, Vol. 4, 585–595, October, 1999, Copyright ©1999 by Cell Press

PPARγ Is Required for Placental, Cardiac, and Adipose Tissue Development

Yaacov Barak,* Michael C. Nelson,*† Estelita S. Ong,*† Ying Z. Jones,‡ Pilar Ruiz-Lozano,§ Kenneth R. Chien,§ Alan Koder,* and Ronald M. Evans*†‖
*Gene Expression Laboratory
†Howard Hughes Medical Institute
The Salk Institute
10010 North Torrey Pines Road
La Jolla, California 92037
‡National Center for Microscopy and Imaging Research
§Department of Medicine
Center for Molecular Genetics
UCSD–Salk Program in Molecular Medicine
University of California, San Diego
La Jolla, California 92093

Summary

The nuclear hormone receptor PPARγ promotes adipogenesis and macrophage differentiation and is a primary pharmacological target in the treatment of type II diabetes. Here, we show that *PPAR*γ gene knockout results in two independent lethal phases. Initially, *PPAR*γ deficiency interferes with terminal differentiation of the trophoblast and placental vascularization, leading to severe myocardial thinning and death by E10.0. Supplementing *PPAR*γ null embryos with wild-type placentas via aggregation with tetraploid embryos corrects the cardiac defect, implicating a previously unrecognized dependence of the developing heart on a functional placenta. A tetraploid-rescued mutant surviving to term exhibited another lethal combination of pathologies, including lipodystrophy and multiple hemorrhages. These findings both confirm and expand the current known spectrum of physiological functions regulated by PPARγ.

Introduction

The nuclear hormone receptors comprise an extended family of transcription factors that utilize ligand-borne signals to regulate genes governing various aspects of eukaryote homeostasis, development, and reproduction (Kastner et al., 1995; Mangelsdorf et al., 1995). Peroxisome proliferator–activated receptors (PPARs) α, γ, and δ constitute a subfamily of nuclear receptors implicated in the control of various aspects of lipid metabolism (Kliewer et al., 1994; Forman et al., 1997). PPARα upregulates the expression of enzymes catalyzing fatty acid oxidation in tissues such as the liver and the heart in response to endogenous ligands or synthetic peroxisome proliferators (Isseman and Green, 1990; Lee et al., 1995). PPARγ, on the other hand, was shown to enhance cellular processes involving lipid accumulation, such as adipogenesis and macrophage foam cell formation (Tontonoz et al., 1994a, 1998). When stimulated by natural or synthetic ligands, PPARγ drives lipid build-up in target tissues through the induction of genes mediating fatty acid uptake, metabolism, and storage (Tontonoz et al., 1994b, 1998; Schoonjans et al., 1996; Sears et al., 1996). A versatile array of ligands for PPARγ includes the natural eicosanoid 15-deoxy-$\Delta^{12,14}$-prostaglandin J_2, endogenous constituents of oxidized LDL (oxLDL) particles such as 9- and 13-HODE, as well as the synthetic thiazolidinedione (TZD) compounds (Forman et al., 1995; Lehmann et al., 1995; Kliewer et al., 1995; Nagy et al., 1998). TZDs, which bind to the receptor and activate it at nanomolar conentrations, are drugs prescribed for the treatment of type II diabetes and insulin resistance (Forman et al., 1995; Lehmann et al., 1995). They thus provide a plausible link between the induction of physiological PPARγ targets and systemic insulin sensitization (Spiegelman and Flier, 1996).

PPARs belong to a subclass of nuclear hormone receptors that, like the retinoic acid, vitamin D, and thyroid hormone receptors, execute their transcriptional functions as heterodimers with the retinoid X receptor (RXR) (Kliewer et al., 1992a, 1992b). Ample experimental evidence suggests that PPAR–RXR heterodimers serve as the core signaling units. These include the demonstration of high-affinity heterodimerization necessary for DNA binding in vitro (Kliewer et al., 1992b); the efficacy of RXR-specific ligands in promoting typical PPARγ activities in cultured cells, such as adipogenesis and macrophage differentiation, alone and in synergy with PPARγ ligands (Mukherjee et al., 1997; Tontonoz et al., 1997, 1998); and the ability of RXR-specific ligands to relieve symptoms of insulin-resistance and type II diabetes in animals (Mukherjee et al., 1997).

The involvement of PPARγ in key metabolic processes pertaining to lipid homeostasis in clinically important situations such as obesity, type II diabetes, and atherosclerosis prompted us to establish a knockout animal model to critically assess its functions. We report here the generation of *PPAR*γ-deficient mice and the discovery of unanticipated essential roles of the receptor during pre- and postnatal development. First, PPARγ is required for epithelial differentiation of trophoblast tissue, which proves critical for proper placental vascularization. These defects lead to myocardial thinning, which can be fully circumvented through selective rescue of the placental pathology, thus revealing a novel functional relationship between the placenta and the developing heart. These fetopathologies share broad similarities with defects in mutants for *RXR*α, alone and in combination with *RXR*β, suggesting that the *RXR* deficiency phenotypes arise primarily from a failure to execute PPARγ functions. Finally, a *PPAR*γ null mouse surviving to term following placental reconstitution exhibited a phenotypic array that included lipodystrophy, fatty liver, and hemorrhages, with fatal consequences during the first week of life. Together these findings identify multiple novel roles for PPARγ, in conjunction

‖To whom correspondence should be addressed (e-mail: evans@salk.edu).

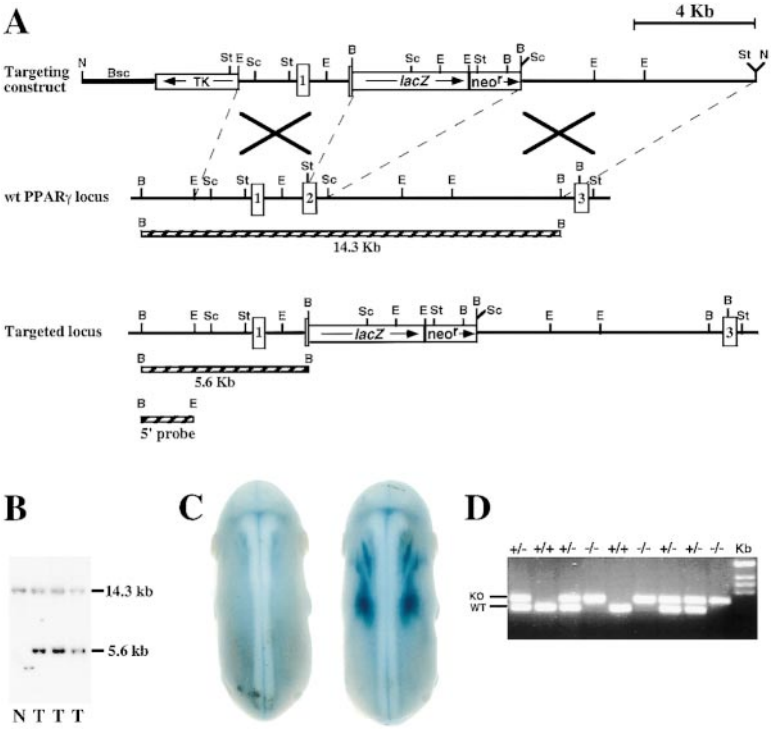

Figure 1. Strategy and Analysis of *PPAR*γ Gene Targeting

(A) *PPAR*γ targeting strategy. A *PPAR*γ targeting construct (top, see the Experimental Procedures for details) was introduced into the genomic *PPAR*γ locus (middle), yielding homologous recombinant loci (bottom). Southern blot analysis strategy (patterned bars below the corresponding genomic structures) is indicated. Restriction sites: B, BamHI; E, EcoRI; N, NotI; Sc, SacI; St, StuI.

(B) Southern blot. Analysis of 5′ homologous integration (see [A] for restriction and size information) reveals appropriate targeting in three of the ES clones (T), as opposed to normal cells (N).

(C) *PPAR*γ-specific targeted allele expression. X-GAL staining detects β-galactosidase expression in the nascent interscapular brown fat pad of E14.5 *PPAR*$\gamma^{+/-}$ (right), but not wild-type embryo (left), recapitulating the abundant expression of *PPAR*γ in this tissue.

(D) PCR analysis of embryos from a *PPAR*$\gamma^{+/-}$ cross. Bottom band (~200 bp), wild-type allele; top band (~230 bp), null allele (KO). Deduced genotypes are indicated on top. Kb, 1 Kb ladder.

with its coreceptor RXR and their ligands, in embryonic and perinatal development.

Results

Embryonic Lethality of *PPAR*γ Null Mice

We mutated the *PPAR*γ gene by in-frame insertion of a *lacZ*-neomycin resistance cassette into the second coding exon, just upstream of the DNA-binding domain (Figure 1A). This knockout strategy eliminates both DNA-binding and ligand-binding functions of PPARγ, concomitantly generating a reporter that faithfully recapitulates its expression pattern. Embryonic stem cells carrying the mutant allele were confirmed by Southern blot analysis (Figure 1B) and subsequently used to derive germline chimeras. Successful targeting of the *PPAR*γ locus and functional utility of the *lacZ* reporter are demonstrated by whole-mount β-galactosidase assays. At E14.5, conspicuous β-gal activity is detected only in embryos carrying a targeted allele and is specific to the interscapular brown fat pad (Figure 1C), which is the first tissue expressing substantial amounts of *PPAR*γ during embryogenesis (Braissant and Wahli, 1998).

Genotype analysis (see Figure 1D) indicates that crosses of one wild-type (+/+) and one heterozygous (+/−) parent yield the expected approximately 50% frequency of *PPAR*$\gamma^{+/-}$ offspring. The heterozygotes are fully developed and fertile and lack external symptoms of disease. Intercrosses of *PPAR*$\gamma^{+/-}$ mice result in the expected approximately 1:2 ratio between wild-type and heterozygous progeny, but no live null (−/−) pups (Table 1). Likewise, no homozygous null embryos can be detected at gestational day 12.5 (E12.5) and beyond. At E9.5 or earlier, *PPAR*$\gamma^{-/-}$ embryos are viable and are recovered at a Mendelian ratio of approximately 25% (Table 1). These embryos have undergone normal chorioallantoic fusion (see Figure 3C) and are externally indistinguishable from their wild-type and heterozygous littermates in both size and gross morphology. All *PPAR*γ-deficient embryos recovered after E9.5 are dead and exhibit progressive necrosis, identifying the narrow temporal window at which this nuclear receptor becomes indispensable.

PPARγ Regulates Essential Placental Functions

The finding that PPARγ is essential as early as E10.0 was unanticipated, since previous reports (Kliewer et al., 1994; Braissant and Whali, 1998), as well as our own whole-mount β-gal staining of hetreozygous embryos (data not shown), failed to detect expression of this gene in embryonic tissues earlier than E14.5. However, our retrospective expression analysis revealed high levels of *PPAR*γ and/or its targeted *lacZ* in the placenta (Figure

Table 1. Embryonic Lethality of *PPAR*γ Null Mice

Stage	Number of Litters	+/+	+/−	−/−
P21	36	59	142	0
E16.5	1	3	4	0
E14.5	1	2	5	0
E12.5	1	2	6	0
E11.5	3	4	14	9[a]
E10.5	1	3	4	2[a]
E10.0	2	8	8	5[a]
E9.5	27	74	116	57
E8.5	1	2	5	2

[a] *PPAR*$\gamma^{-/-}$ embryos isolated between E10.0 and E11.5 have pale yolk sacs. Fetuses are dead and progressively necrotic.

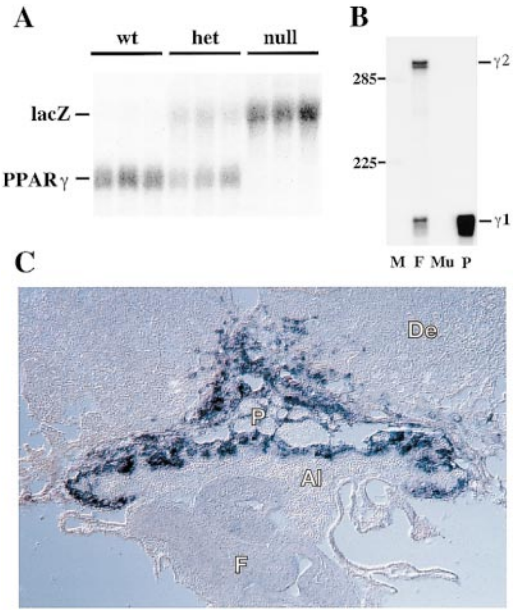

Figure 2. Placental Expression of *PPARγ*

(A) Northern blot analysis. Genotype-specific expression pattern of *PPARγ* and *lacZ* in placentas of heterozygote cross E9.5 progeny. The blot, containing 5 μg total RNA per lane, was hybridized simultaneously with probes for *PPARγ* and *lacZ* (hybridization signals indicated). Quantitative normalization was confirmed using a probe for the placenta-specific *Mash-2* gene (data not shown).

(B) RNase protection assay. Protection of alternative RNA fragments derived from the *PPARγ2* (γ2; 292 nucleotides) and *PPARγ1* (γ1; 187 nucleotides) isotypes reveals tissue-specific expression patterns. Fat tissue (F, 3 μg RNA) contains both isoforms, and muscle (Mu, 20 μg) lacks detectable expression of *PPARγ*, whereas the placenta (P, 10 μg) expresses exclusively *PPARγ1*, at levels comparable to those in fat. Length of ribomarkers (M) in nucleotides is shown on the left.

(C) In situ hybridization. *lacZ* transcripts (dark blue) are expressed throughout the placenta (P) in *PPARγ*$^{+/-}$ *embryos. PPARγ* (data not shown) exhibits an identical hybridization pattern in both wild-type and heterozygous placentas. Al, allantoic cavity; De, decidual tissue; F, fetus.

2A), consistent with the notion that death around E9.5 is a common consequence of defects in extraembryonic tissues (Copp, 1995). Robust *PPARγ* expression can be detected in the placenta at least as early as E8.5 and throughout the remainder of gestation (data not shown), with *PPARγ1* and not the adipocyte-specific *PPARγ2* being the exclusive placental mRNA isoform (Figure 2B). Within the placenta *PPARγ* (or interchangeably, *lacZ*) expression is restricted to the diploid trophoblast lineages, including the spongiotrophoblast and the entire labyrinthine trophoblast (Figure 2C). Residual expression levels can be detected in some secondary giant cells. Notably, neither PPARγ nor *lacZ* are expressed in the fetal endothelium permeating the presumptive labyrinth.

The placenta-restricted expression of *PPARγ* and the lethal effect of placental dysfunction at E9.5 and beyond provide a plausible mechanistic explanation for the early death of homozygous null embryos. To test this prediction, we generated aggregation chimeras between wild-type tetraploid embryos and diploid embryos derived from crosses of *PPARγ*$^{+/-}$ parents (Nagy et al., 1990). The tetraploid morulas fail to contribute to the embryo proper, which is therefore derived entirely from the diploid partner of the chimera. Yet, the tetraploid cells maintain an unrestricted potential to develop into the extraembryonic lineages, such that the placenta is invariably *PPARγ*$^{+/+}$. Thus, if embryonic lethality of *PPARγ* null embryos at E10.0 is the outcome of placental defects, it should be rescued by the tetraploid partners.

Genotype determination of the resulting chimeras confirms this hypothesis. Viable *PPARγ* null ↔ tetraploid chimeras were recovered at E12.5 (two mutants out of a total of five), E15.5 (one out of ten), and at birth (one of six). These data demonstrate unequivocally that the essential functions of PPARγ during embryonic development are restricted to the placenta. As discussed below, while the rescued embryos appear viable, a second lethal phase was discovered in the perinatal period.

Vascular Anomalies in *PPARγ* Null Placentas and Their Reiteration in *RXR* Null Mice

The unchanged expression pattern of placenta-specific markers (data not shown) suggests that PPARγ is dispensable for the establishment of trophoblast lineage identity. However, the establishment and maintenance of the fetal and maternal vascular networks in *PPARγ* null placentas are abnormal (Figure 3). First, while fetal vessels (fv) permeate the presumptive labyrinth of wild-type and heterozygous placentas by E9.5 (Figures 3A and 3B), they rarely invade the mutant labyrinth (Figure 3C). Second, maternal blood sinuses (mv), which in the normal placenta are compact and well-defined (Figure 3A), are frequently dilated, ruptured, and consequently adjoined within *PPARγ*$^{-/-}$ placentas, sometimes forming a continuous blood pool throughout the entire zone (Figure 3C). Moreover, maternal erythrocytes, which are normally confined strictly to the sinuses (see Figure 3A), are observed throughout the cytoplasms of cells in the mutant junctional zone (JZ; Figure 3C), reflecting overt erythrophagocytic activity of the trophoblasts lining the maternal sinuses in the mutant (Figure 3D). These maternal vascular defects are intermediary in *PPARγ*$^{+/-}$ placentas (Figure 3B).

Ultrastructural analysis of normal placental tissue reveals that by E9.5 a significant portion of the labyrinthine trophoblast establishes the characteristic three cell–layered (hemotrichorial) epithelial barrier between maternal blood pools and the fetal endothelium (Figures 3E and 3F). Adjacent layers of this epithelial barrier are tightly packed and intimately associated with a compacted fetal allantoic endothelium (en), both at the deepest vascular protrusions (Figure 3E) and at the placenta–allantois interface (Figure 3F). Each of the layers (designated I, II, and III, counting from the maternal side toward the fetal vessels) acquires typical characteristics, which become further accentuated with time (Jollie, 1964; Enders, 1965).

In contrast, in *PPARγ* null placentas, the invaginating chorionic villi are surrounded by excessively thick trophoblast tissue (Figure 3H), which only faintly resembles the differentiated barrier and retains the ultrastructural characteristics of the early labyrinthine parenchyma

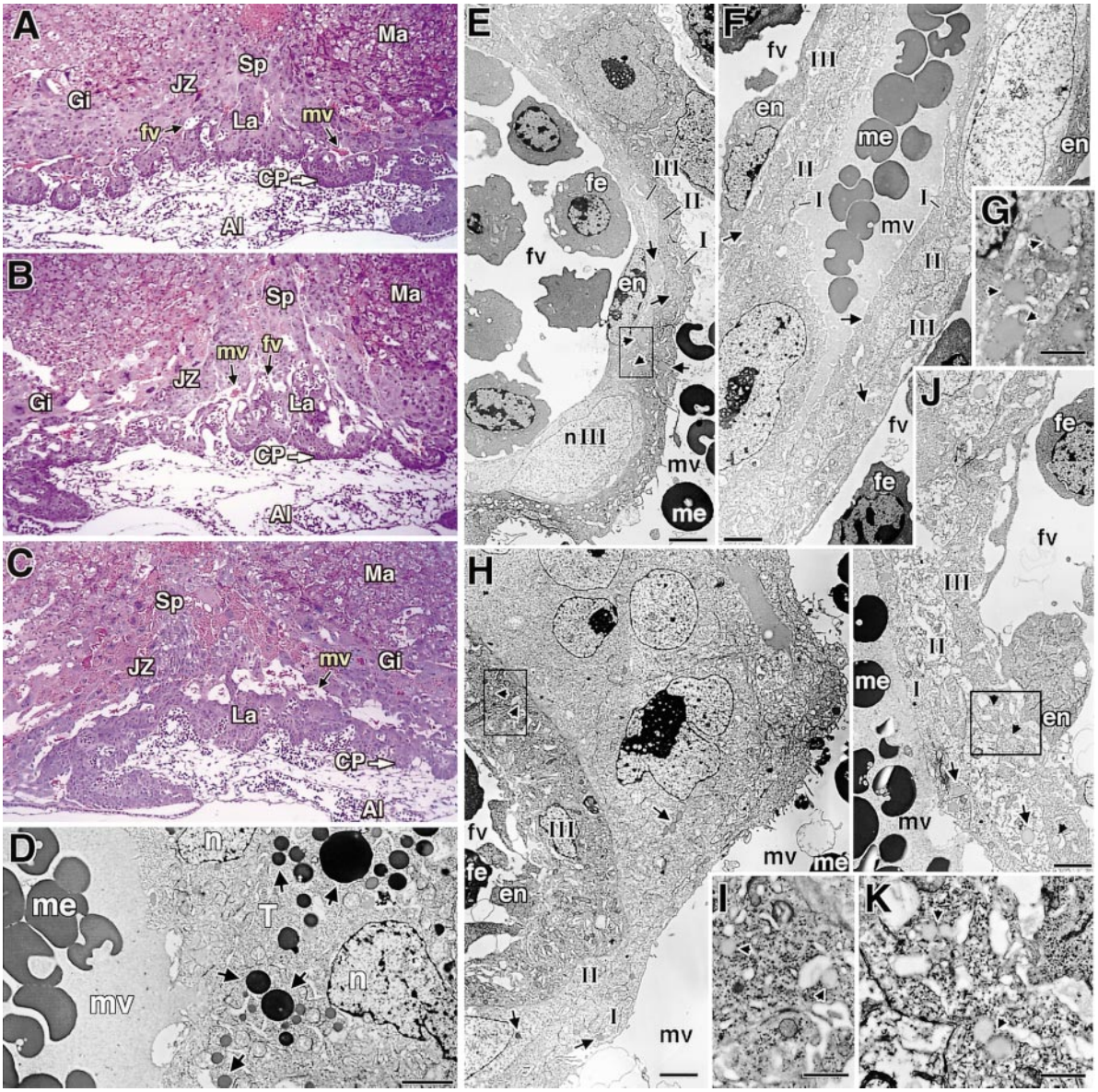

Figure 3. Histological and Ultrastructural Studies of Wild-Type and Mutant Placentas at E9.5

(A–C) Hematoxylin and eosin stained 5 μm paraffin sections of *PPARγ*$^{+/+}$ (A), *PPARγ*$^{+/-}$ (B), and *PPARγ*$^{-/-}$ (C) placentas. Note the dilated maternal vessels (mv) and the conspicuous amounts of maternal erythrocytes (red dots) within the trophoblast in the junctional zone (JZ) of the mutant placenta (C) and to a lesser extent the heterozygous one (B). Evident in (C) are the abnormal thickening of the mutant chorionic plate (CP) and poor impregnation of the mutant presumptive labyrinth (La) by fetal vessels (fv, containing blue stained nucleated fetal erythrocytes). Al, allantoic cavity; Gi, secondary giant trophoblast; Ma, (maternal) decidua; Sp, spongiotrophoblast.

(D) Phagocytosis of maternal erythrocytes in *PPARγ*$^{-/-}$ placenta. Shown is an electron micrograph of a typical trophoblast cell in the mutant junctional zone. Arrows indicate phagocytic vesicles containing maternal erythrocytes at different stages of ingestion. mv, maternal blood vessel; N, trophoblast cell nucleus.

(E–K). Ultrastructure of the trophoblast barrier. Wild-type trophoblast within the labyrinth (E) and at the placenta–allantois interface (F). Note the highly organized nature, compaction, close contact, and distinctive appearance of the hemotrichorial layers (Roman numerals) and fetal endothelium (en). Lipid droplets are scattered in layers I and II (arrows) and clustered in layer III (arrowheads; magnified in [G]). fe, fetal erythrocyte; nIII, cell nucleus in layer III. (H) Poorly differentiated *PPARγ*$^{-/-}$ chorionic villus. Cells are extremely thick and distinctive layer characteristics are diminished. Scarce lipid droplets in presumptive layers I and II (arrows) and a pair of miniscule lipid droplets in layer III (arrowheads; magnified in [I]) are indicated. (J) *RXRα*$^{-/-}$ labyrinthine barrier. The trophoblast epithelium is not as compact as in the wild-type, and the fetal endothelium (en) is detached from layer III (compare to [E]). Lipid droplet distribution and size in layers I and II (arrows) are similar to wild-type placentas (compare to [E] and [F]), while those in layer III (arrowheads; magnified in [K]) are significantly fewer and smaller. Scale bars: (D–F, H, and J), 3 μm; (G, I, and K), 1 μm.

(compare Figure 3H to Figures 3E and 3F). The fetal endothelium (en) does not establish close contact with the *PPARγ* null trophoblast and remains indistinguishable from the loose endothelial mesh of the allantois (Figure 3H). Overall, the maturation block of *PPARγ*$^{-/-}$ labyrinthine trophoblast, in combination with the failure to establish placental vasculature, most likely severely compromise maternal–fetal exchange functions resulting in early lethality.

The role of RXRs as coreceptors for the transcriptional activity of PPARγ sets the prediction that the phenotype of *RXR*-deficient mice should encompass that of *PPARγ* mutants. Indeed, deficiency for *RXRα*, which is the predominant RXR species in the placenta (Sapin et al., 1997a), leads to multiple vascular defects in the organ (Sapin et al., 1997b). We find manifestations of these defects in *RXRα* null placentas as early as E9.5, including reduced fetal vessel permeation, phagocytosis of maternal blood cells (data not shown), incomplete epithelialization of the barrier, and looser endothelial trophoblast contacts (compare Figure 3J with 3E). Each of these defects has a typically more severe counterpart in *PPARγ* null placentas.

This attenuated phenocopy is a likely reflection of genetic redundancy between RXR isoforms. The markedly increased severity of placental defects in *RXRα*/*RXRβ* double mutants (Wendling et al., 1999), as well as their earlier death (~E10.0) compared to E12.5–E16.5 in the case of mice deficient for *RXRα* alone, is consistent with this notion. Residual levels of RXRβ in the placenta (data not shown) conceivably support some PPARγ function in *RXRα* mutants to provide limited phenotypic alleviation relative to a complete loss of PPARγ activity.

Lipid Accumulation Deficits in *PPARγ* and *RXRα* Null Placentas

The labyrinthine barrier of rodents harbors an abundance of large, densely clustered lipid droplets crowded along the basolateral surface of layer III (Jollie, 1964). Electron micrographs of E9.5 placentas reveal precursors for these droplets in wild-type and *PPARγ*$^{+/-}$ trophoblast (see arrows in Figures 3E–3G). These droplets, whose average diameter is 0.7 μm at this stage, are visible throughout the three layers of the trophoblast barrier but are concentrated within layer III. In contrast, lipid droplets are extremely scarce in the *PPARγ*-deficient presumptive labyrinth, and the rarely detected ones are much smaller than in the wild-type barrier (~0.2 μm diameter; Figures 3H and 3I, arrowheads).

Similarly, *RXRα*-deficient placentas at E9.5 also display a dramatic decrease in lipid droplet abundance and diameter (~0.45 μm) in layer III, although not quite to the extent observed in *PPARγ* mutants (compare Figure 3K with Figures 3G and 3I). This finding agrees with the aforementioned notion of attenuated PPARγ-deficiency in *RXRα*$^{-/-}$ placentas, as well as with an earlier report of substantial reduction in the number of lipid droplets in layer III of *RXRα*$^{-/-}$ placentas at E12.5 (Sapin et al., 1997b). Thus, PPARγ/RXR heterodimers regulate trophoblast lipid accumulation in a manner that may be analogous to their actions in adipose tissue and macrophages.

Placental Defects Elicit Myocardial Thinning in *PPARγ* Null Embryos

Prior to their death, *RXR* null embryos exhibit severe thinning of the ventricular wall, trabeculae, and septum (Kastner et al., 1994, 1997; Sucov et al., 1994). Given the resemblance between the placental phenotypes of *RXR* and *PPARγ* null embryos, we wondered whether such a cardiac phenotype might be linked to *PPARγ* deficiency. Histological examination of *PPARγ*$^{-/-}$ embryos at E9.5 confirmed this suspicion, revealing severe ventricular hypoplasia (arrows) and degeneration of the trabecular zone (T) (compare Figures 4A and 4B). The severity of this defect markedly exceeds the one observed in *RXRα* null embryos at the same stage (Kastner et al., 1994; Sucov et al., 1994), though it is not as profound as in compound *RXRα*/*RXRβ* null embryos (Kastner et al., 1997).

Acquisition of contractile properties by cardiomyocytes is delayed at the subepicardial layer of the ventricle until E16.5, while progressing earlier in the inner ventricular layers and the trabeculae (Kastner et al., 1997). In agreement with this observation, we find that wild-type ventricular subepicardial myocytes have not yet differentiated at E9.5 and at most harbor occasional loose myofilament bundles (MF; Figure 4C). In contrast, in *RXRα* null embryos, these cells exhibit precocious differentiation, which becomes overt in *RXRα*/*RXRβ* compound null embryos and is linked to reduced cell proliferation in the ventricular wall (Kastner et al., 1997). This phenomenon is reiterated in *PPARγ*$^{-/-}$ embryos (Figure 4D), where frequent tandem sarcomers are observed, separated by multiple Z lines (Z), crossing cell boundaries through intercalated discs (ID). Thus, a similar spectrum of cardiomyopathies is shared by *PPARγ* and *RXR* null mice, including premature cardiomyocyte differentiation and ventricular hypoplasia.

In addition to thinning and early differentiation of the ventricles, numerous mitochondria in the subepicardial cells of *PPARγ* null embryos are severely inflated and irregularly shaped (compare Figures 4E and 4F). This feature could represent a symptom of mitochondrial cardiomyopathy—a syndrome associated with the adaptive regulation of mitochondrial functions in response to metabolic deprivation (Sengers et al., 1984). Such an interpretation is in line with earlier findings describing global downregulation of transcripts related to energy metabolism in *RXRα* null fetuses (Ruiz-Lozano et al., 1998). Since *PPARγ* expression is restricted to the placenta prior to E14.5 (see above), we postulated that placental insufficiency could be directly underlying the cardiac defects in *PPARγ* (and *RXR*) null mice. This idea was further fueled by the recognition of the cardiomyocyte nonautonomous nature of the ventricular phenotype in *RXRα*$^{-/-}$ embryos (Chen et al., 1998; Tran and Sucov, 1998).

We tested this hypothesis by examining the hearts of *PPARγ* null ↔ tetraploid chimeras, in which the placental defects are genetically cured (see above). These embryos, which are otherwise *PPARγ* deficient, exhibit no evidence of hypoplastic ventricular wall or septum at either E12.5 (compare Figure 5B to Figure 5A) or E15.5 (Figures 5C and 5D). Therefore, ventricular thinning in *PPARγ*$^{-/-}$ embryos is a direct consequence of placental

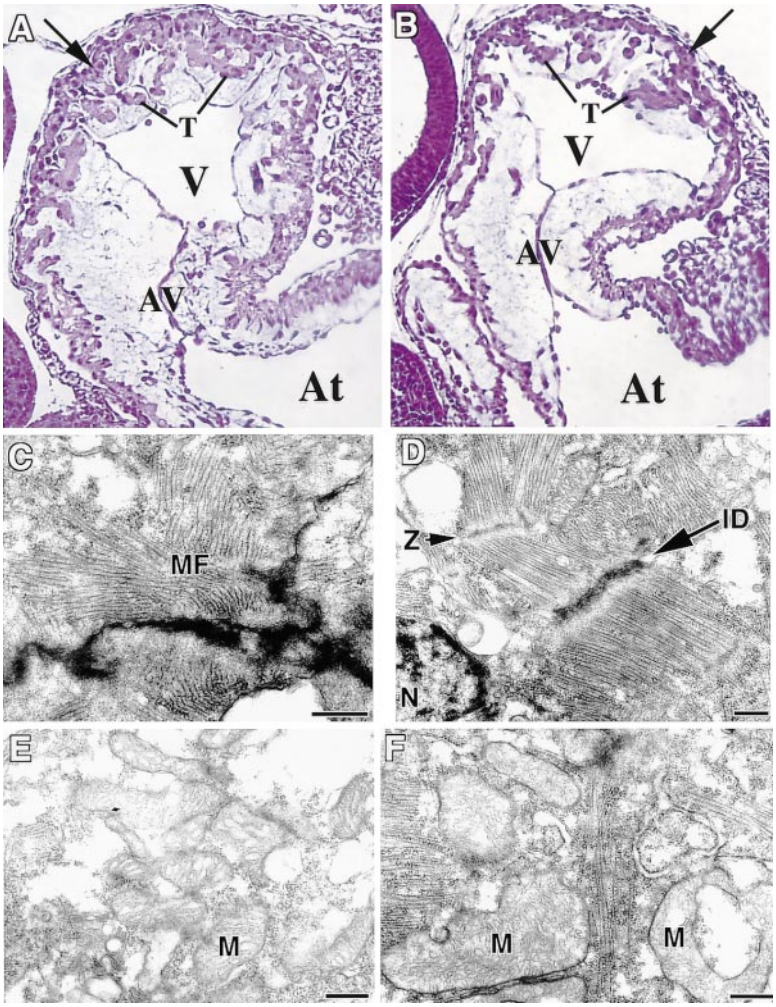

Figure 4. Ventricular Chamber Defects in *PPAR*γ Null Embryos

(A and B) Hearts of wild-type (A) and *PPAR*$\gamma^{-/-}$ (B) embryos at E9.5. Note the severe thinning of the compact zone of the ventricular myocardium (arrows) and degenerated trabeculae (T) in the mutant. At, atrial chamber; V, ventricular chamber; AV, atrioventricular canal bordered by endocardial cushions.

(C–F) Electron microgarphs of ventricular subepicardial myocytes. A myofilament bundle (MF) characteristic of the wild-type cardiomyocyte (C), stands in sharp contrast to the mutant subepicardium, which contains abundant sarcomers, such as the one in (D), separated by Z lines (Z) and intercalated discs (ID). N, cell nucleus. (E) Normal cardiac mitochondria in wild-type embryos, vs. (F) A cluster of ventricular mitochondria with extreme aberrations in size (left M) and shape (right M) in *PPAR*γ null embryos. Scale bars, 0.5 μm.

dysfunction, highlighting the existence of an apparently unrecognized but crucial placenta–heart axis.

Lipodystrophy, Fatty Liver, and Multiple Hemorrhages in *PPAR*γ Null Mice

All *PPAR*γ null ↔ tetraploid chimeras retrieved between E10.0 and term were viable, indicating that, other than its role in the placenta, PPARγ is not essential during embryogenesis. Indeed, a viable *PPAR*γ-deficient pup was recovered through tetraploid rescue. This pup was a runt, yet throughout the first 4 postnatal days (P0–P4.0) maintained a body weight of 70% relative to its *PPAR*$\gamma^{+/-}$ chimeric sibling. However, starting at P5, its health deteriorated rapidly, as manifested by dehydration, actual weight loss (~20% per day), and lethargy, despite active suckling. The two pups were subsequently sacrificed for analysis at P6.5.

The mutant pup exhibited a striking absence of all types of adipose tissue. Thus, while the *PPAR*$\gamma^{+/-}$ ↔ tetraploid chimera harbored a conspicuous brown adipose tissue in the interscapular region (Figure 6A, BAT), no sign of brown fat could be detected at the same location in the mutant (Figure 6B, asterisk). Moreover, both white fat pads and subcutaneous fat started to emerge in the heterozygote pup, while completely absent in the mutant (data not shown). These observations provide direct evidence that PPARγ is indispensable for adipogenesis in vivo. Notably, although terminally differentiated adipose tissue is eventually absent, there appears to be an initial commitment to the brown fat lineage in *PPAR*γ mutants. This is manifested as an interscapular β-gal expressing tissue, which at E15.5 is still indistinguishable between *PPAR*$\gamma^{+/-}$ (Figure 6C) and null embryos (Figure 6D). Thus, PPARγ is not required for the early establishment of brown adipose tissue, but rather for its elaboration.

In addition, the mutant pup exhibited a severely fatty liver (Figure 6F, Li). The organ was very pale and distended, with a significant increase in individual cell size and the cytoplasmic accumulation of multiple lipid droplets (Figure 6H), as compared with the normal size and cytoplasmic staining of heterozygous hepatocytes (Figures 6E and 6G). Therefore, the loss of PPARγ leads to an abnormal build-up of hepatic lipid stores—a phenomenon shared with other models of lipodystrophy (Moitra et al., 1998; Shimomura et al., 1998).

The defects in the *PPAR*γ null pup extend to additional organs, including severe intestinal bleeding (Figure 6F,

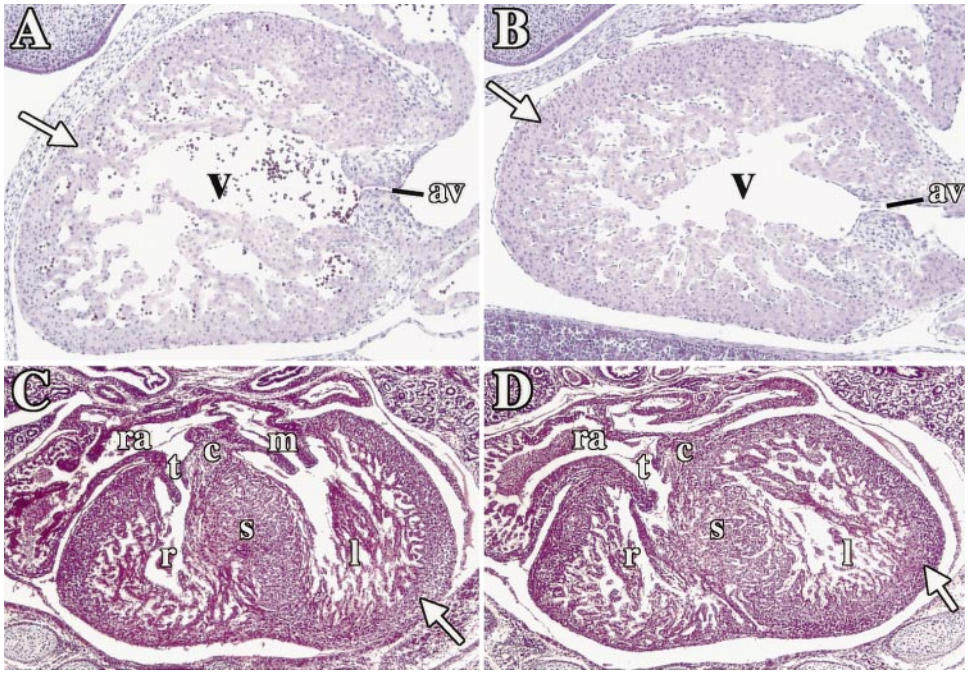

Figure 5. Normal Cardiac Development in *PPAR*γ Null Tetraploid Chimeras

Sagital view of the cardiac ventricles of E12.5 *PPAR*$\gamma^{+/-}$ (A) and null (B) tetraploid chimeras, and transverse sections through the ventricles of E15.5 *PPAR*$\gamma^{+/-}$ (C) and null (D) chimeras. No differences can be detected in the thickness of the ventricular wall (as well as the septum in [C] and [D]) between both genotypic settings. Arrows, compact zone of the ventricular wall; av, atrioventricular valve; c, endocardial cushion; l, left ventricle; m, mitral valve; r, right ventricle; ra, right atrial chamber; s, interventricular septum; t, tricuspid valve; V, ventricular chamber.

In) and numerous focal hematomas throughout the brain (data not shown). While the primary cause of these hemorrhages is unclear at this point, they are likely to contribute to the rapid deterioration of the mutant pup. Together with the body of data presented above, they implicate PPARγ as impacting on development and organogenesis in a surprisingly diverse fashion.

Discussion

PPARγ and Adipogenesis

PPARγ has emerged in recent years as a pivotal regulator of lipid metabolism in various tissues. It has been tightly linked to the induction of adipogenesis (Tontonoz et al., 1994a; Forman et al., 1995) and inferred as a systemic insulin sensitizer through its mediation of antidiabetic drug activity (Forman et al., 1995; Lehmann et al., 1995). PPARγ appears to play an equally important role in the differentiation of macrophages into foam cells and in the mechanisms of oxidized LDL clearance and accumulation by macrophages (Nagy et al., 1998; Tontonoz et al., 1998). Here, using homologous recombination, we demonstrate that a *PPAR*γ mutant mouse is deficient for all forms of fat. Thus, we establish that PPARγ promotes adipogenesis not only in cultured cells (Tontonoz et al., 1994a; Forman et al., 1995) but also in vivo.

Interestingly, a PPARγ-expressing domain, which likely represents an early predecessor of the brown fat pad, can be identified in *PPAR*γ null embryos. This observation indicates that PPARγ is not required for the initial stages of adipogenesis involving lineage commitment. However, the absence of discernable adipose tissue in newborn mutants suggests that the ultimate fate of the committed tissue is dependent upon a functional *PPAR*γ gene product. This implication is in line with the postulated hierarchical position of PPARγ in the adipogenic program in vitro (Spiegelman and Flier, 1996), which is downstream of earlier adipogenic markers, such as C/EBPβ, but precedes the emergence of late adipogenic factors like C/EBPα.

The *PPAR*γ-deficient mouse develops fatty liver at birth, reminiscent of established animal models and clinical cases of lipodystrophy (Seip and Trygstad, 1996; Moitra et al., 1998; Shimomura et al., 1998). It is postulated that this syndrome is precipitated primarily by de novo lipogenesis in hepatocytes, presumably in response to insulin resistance-induced hyperinsulinemia in the lipodystrophic setting (Shimomura et al., 1998). We suggest that a similar chain of events, combined with a failure to store and process triglycerides from maternal milk in adipose tissue, lead to the development of fatty liver in the *PPAR*γ null mouse.

Placental Functions of PPARγ

We elucidate here a previously unexpected essential role for PPARγ in the structure and function of the chorioallantoic placenta. This conclusion is supported by three lines of evidence. First, genetic ablation of *PPAR*γ demonstrates that its presence is indispensable at the earliest developmental stage requiring a functional placenta—E9.5. Second, at the time of lethality, and for at least 3–4 additional gestation days, the only embryonic tissue expressing detectable levels of *PPAR*γ is the

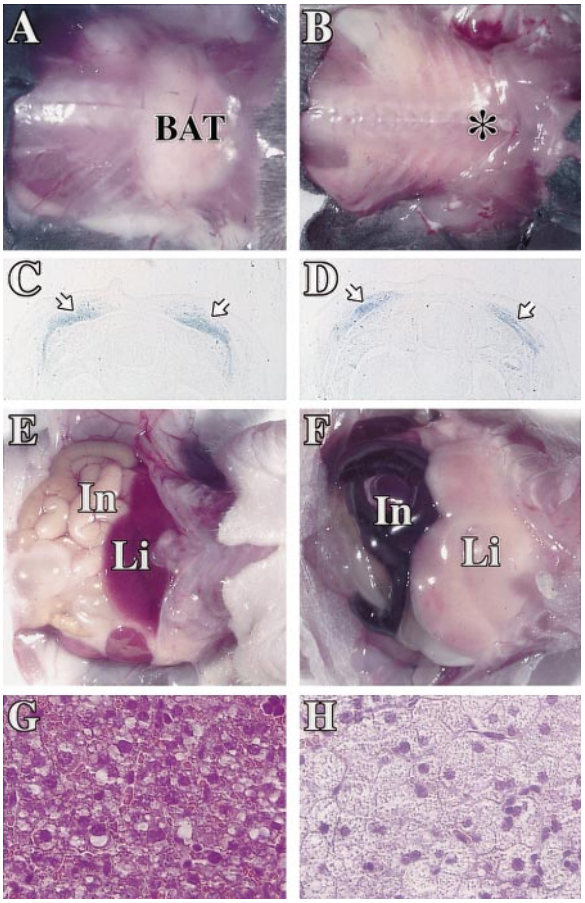

Figure 6. Lipodystrophy, Fatty Liver, and Intestinal Hemorrhage in *PPAR*γ Null Mice

(A and B) Rear views of *PPAR*$\gamma^{+/-}$ (A) and *PPAR*γ null (B) tetraploid-rescued pups. Note the presence of a conspicuous brown adipose tissue (BAT) in the heterozygote and its complete absence in the null (an asterisk marks the projected location of the missing tissue).

(C and D) Transverse sections of whole-mount X-gal stained *PPAR*$\gamma^{+/-}$ (C) and null (D) tetraploid chimeras at E15.5. Both pups exhibit an essentially similar staining pattern, indicative of the initial establishment of a *PPAR*γ-expressing brown adipose lineage.

(E and F) Visceral views of the *PPAR*$\gamma^{+/-}$ (E) and *PPAR*γ null (F) rescued pups. The liver (Li) of the mutant is extremely pale and distended. The intestine (In) is black, as a result of a massive bleeding into its lumen (data not shown).

(G and H) Histological sections of the livers shown in (C) and (D), respectively. Note the abnormally hypertrophic, lipid-laden appearance of the mutant hepatocytes (H).

placenta. Finally, and most importantly, *PPAR*γ null embryos are rescued by tetraploid chimeras, demonstrating that PPARγ dependency resides within extraembryonic tissues.

At the whole tissue level, the vascular structures of *PPAR*γ null placentas are disarrayed. Fetal vessels only rarely traverse the chorionic plate into the presumptive labyrinth, and the few that succeed fail to flank the maternal blood pools. This anomaly alone most likely compromises maternal–fetal exchange. The observed vascular defects are clearly trophoblast autonomous and vessel nonautonomous, considering the trophoblast-restricted expression of PPARγ, as well as the successful phenotypic rescue by tetraploid chimeras. Moreover, all other vascular processes in the null embryos are normal, including the establishment of yolk sac circulation, the formation of vitellin vessels and major arteries, and chorioallantoic fusion. Therefore, PPARγ-dependent trophoblast functions are obligatory for placental vascularization.

The nature of such functions is suggested by the ultrastructural features of the trophoblast in the *PPAR*γ-deficient presumptive labyrinth. This tissue fails to undergo the terminal differentiation associated with its barrier functions, resulting in a probable decrease in metabolite exchange. Shutoff of the syncytial/epithelial program may have adverse effects on trophoblast–endothelium interactions, as well as on the integrity of the trophoblast-lined maternal blood sinuses, thus potentially contributing to the observed vascular defects. It is noteworthy that PPARγ is expressed in other epithelial cells, such as those of the mammary gland, the colonic mucosa, and the urinary bladder (Jain et al., 1998; Saez et al., 1998), as well as additional secretory glands (Y. B., unpublished data). It is tempting to speculate a common function for PPARγ in these epithelial tissues and the placenta.

Our data further indicate that PPARγ is required for the accumulation of lipid droplets by the labyrinthine trophoblast. The apparent dependence of this phenomenon on intact PPARγ signaling is consistent with the role of the receptor in coordinating lipid uptake and storage elucidated previously in adipocytes and macrophages (Tontonoz et al., 1994a, 1998; Nagy et al., 1998). It thus expands the range of tissues in which PPARγ is known to regulate these processes.

PPARγ–RXR Relationships In Vivo

This study reveals striking similarities between the *PPAR*γ null and *RXR* null phenotypes. These findings underscore the obligatory role of heterodimerization with RXR for PPARγ signaling in vivo. This conclusion is a natural extension of earlier studies showing RXR-dependence of PPARγ DNA binding and transactivation functions and the potency of RXR-specific ligands in enhancing biological activities mediated typically by PPARγ (Kliewer et al., 1992b; Mukherjee et al., 1997; Tontonoz et al., 1997, 1998). Surprisingly, our observations define the loss of PPARγ signaling as the probable cause of placental, and perhaps also cardiac, defects in *RXR*-deficient mice, replacing earlier candidate partners, such as the retinoic acid receptors or RXR homodimers. Still, we cannot entirely rule out potential contributions to the latter phenotype by additional RXR-dependent nuclear receptors. Such complexity could account for what seem to be earlier and more severe cardiac and placental pathologies in *RXR*α*/RXR*β compound mutants (compare with Kastner et al., 1997; Wendling et al., 1999).

Placental Defects and Thin Myocardial Wall Syndrome

Cardiomyopathies are the most frequent reason for fatalities during the first year of infancy and are probably the leading cause of spontaneous miscarriage, especially at late gestation. According to recent estimates, around 1 in 200 human newborns suffers from a life threatening cardiomyopathy, with around one-third of

these exhibiting a morbidly thin myocardium and/or an incomplete ventricular septum (Friedman, 1988). While, for a small fraction of patients, a cardiac-autonomous congenital defect has been identified as the underlying cause of the disease, the etiology of most cases remains obscure (Chien, 1993; Olson and Srivastava, 1996; Rossant, 1996). Here, we present evidence for the existence of a placenta–heart axis, whose disruption precipitates thin myocardial wall syndrome. The ability to achieve complete reversal of the cardiac phenotype of *PPAR*γ null embryos through selective replacement of their trophoblast lineage by tetraploid chimera methodology supports this notion. Thus, our study suggests that some inborn human cardiomyopathies could be the result of placental abnormalities and, by extension, that PPARγ/RXR heterodimers and their ligands might affect the function of this axis.

Whatever the nature of the critical placental defect is, the heart seems to be the only tissue affected by it, as neither the growth nor the develpoment of other organ systems are compromised in mutant embryos by the original time of death (data not shown). In this context, a previous study found a tissue-specific decrease in the ATP content of ventricular cardiomyocytes from RXRα null embryos relative to wild-type siblings, suggesting failure of the heart to produce sufficient energy in the setting of that mutation (Ruiz-Lozano et al., 1998). Since the *RXR*$\alpha^{-/-}$ ventricular phenotype likely represents an attenuated manifestation of *PPAR*γ deficiency, we suspect that an even more severe metabolic failure of the heart occurs in *PPAR*$\gamma^{-/-}$ embryos. Consistent with this interpretation, we find increased incidence of abnormal mitochondria in ventricular cardiomyocytes from *PPAR*γ null embryos, which could indicate an attempted adaptive response of these cells to energy deficiency, as in classical mitochondrial cardiomyopathies (Sengers et al., 1984). This set of correlations suggests that a metabolic deficit may underlie myocardial thinning in *PPAR*γ and *RXR* null embryos and perhaps also in human embryos exhibiting idiopathic ventricular or septal hypoplasia.

Conclusion

We describe two temporally distinct functions of PPARγ in vivo. First, PPARγ has an obligatory role in adipose tissue formation, and its absence leads to complete lipodystrophy. Second, PPARγ regulates terminal epithelial differentiation of the trophoblast, which, given the ubiquitous expression of PPARγ in epithelia of endocrine and exocrine tissues, could apply to additional organs. Most importantly, we unravel the existence of a previously unrecognized functional link between the placenta and the developing heart, which could shed new light on the origins of congenital cardiomyopathies. Together, these results expand the known spectrum of physiological processes orchestrated by PPARγ, uncovering a broader and more complex role for this nuclear receptor, and by implication its ligands, than previously anticipated.

Experimental Procedures

Generation and Analysis of *PPAR*γ Mutants

A *lacZ-PGKneo* cassette was inserted into genomic *PPAR*γ DNA isolated from 129/Sv strain–derived library upstream of the first zinc finger coding region, generating in-frame fusion between *lacZ* and a short N-terminal fragment of *PPAR*γ. The remainder of that exon and a short piece of flanking intron were concomitantly deleted. A herpes simplex virus *thymidine kinase* gene (*TK*) was attached to the targeting cassette, and the construct was electroporated into the J1 mouse ES line followed by a conventional 7 day positive–negative selection scheme. Surviving colonies were screened for homologous recombination events by Southern blot hybridization of BamHI digested DNA with a probe lying outside the 5′ homology arm (see Figure 1A for maps). Positive clones (7 out of 108) were further verified using a 3′ external probe.

Germline chimeras were derived from four independent targeted clones. PCR genotyping was carried out using one common and two allele-specific oligonucleotides at the 5′ junction of the targeting cassette as follows: AGGCCACCATGGAAAGCCACAGTTCCTC (Common, 3′ part of intron 3); TCCCCACAGACTCGGCACTCA ATGGC (wild type–specific, 3′ portion of exon 4); GCTGGCGAAAG GGGGATGTGCTGCAAG (null-specific, 5′ part of *lacZ*). Genomic DNA (0.5 μg) was amplified through 35 cycles of: 94°C, 20 s; 60°C, 30 s; 72°C, 55 s. Reaction products approximately 200 and approximately 230 bp long represent the wild type and the mutant allele, respectively.

RNA Detection and Analysis

Northern blots, RNase protection, and in situ hybridization were carried out as described (Tontonoz et al., 1998; Barak et al., 1994; Schaeren-Wiemars and Gerfin-Moser, 1993, respectively). An approximately 800 bp BglII fragment from the 3′ part of *PPAR*γ cDNA, not expressed in the null configuration, was used as a probe in Northern blots and in situ hybridization. The RNase protection template covered the *PPARγ2* isoform–specific sequence (Tontonoz et al., 1994b) plus first 187 nucleotides (nt) common to both isoforms. *PPARγ2*-specific protection yielded the expected 292 nt long band, whereas *PPARγ1* was simulated by a 187 nt long protected fragment.

Histology and Electron Microscopy

Whole-mount X-GAL staining is described elsewhere (Hogan et al., 1994). For placenta histology, 5 μm thick sections of paraffin-embedded concepti were stained with hematoxylin and eosin. Genotypic identity of each embryo was determined by the in situ hybridization pattern of adjacent sections with *PPAR*γ and *lacZ*. Placentas hybridizing with either *PPAR*γ or *lacZ* are wild type or *PPAR*γ null, respectively, whereas those hybridizing with both probes are heterozygous. Histology of isolated embryos was carried out using standard procedures.

For electron microscopy, whole E9.5 fetuses or whole E9.5 placentas were fixed overnight in cold phosphate buffer saline (PBS) containing 3% glutaraldehyde. Tissues were washed and equilibrated with 1% osmium tetroxide, followed by overnight staining with 2% uranyl acetate. Samples were washed and dehydrated in ethanol series, infiltrated with Durcupan ACM resin and polymerized for 24 hr at 60°C. Thin sections (100 nm) were cut using a Reichert Ultracut E, stained with lead acetate, and examined using a JEOL 100CX electron microscope at 80 KeV.

Generation of Tetraploid Embryos

Procedure followed a published protocol (Nagy and Rossant, 1993) with some modifications. Briefly, two-cell stage blastomers were recovered from superovulated CB6F1 females fertilized by CB6F1 males. The blastomers were fused in 0.3 M mannitol drops using a CF150 electrofusion apparatus (Biochemical Laboratory Services, Budapest, Hungary), and the resulting tetraploid embryos were incubated overnight at 37°C, 5% CO_2 in KSOM medium. Following two cell divisions, four-cell tetraploid morulas, as well as diploid six- to eight-cell stage morulas recovered freshly from *PPAR*$\gamma^{+/-}$ × *PPAR*$\gamma^{+/-}$ matings were treated with acid Tyrode's solution to remove the zona pellucida. Subsequently, overnight aggregates of one diploid embryo with two tetraploids were assembled in KSOM-covered microdepressions in a cell culture incubator. Aggregation-derived blastocysts were implanted into pseudopregnant ICR females, and chimeric embryos were either recovered for analysis or allowed to develop to term.

Acknowledgments

We thank A. Malchiodi for technical assistance; Drs J. Rossant, V. Sapin, and H. Sucov for valuable discussions and comments on the manuscript; Dr. P. Chambon for communicating *RXR*α/β knockout data prior to publication; Dr. T. Kadowaki for communicating unpublished *PPAR*γ knockout data; Drs J. Rossant and D. Linzer for placenta-specific probes; Dr. S. Pfaff for advice on in situ hybridization and for the use of microscopes and photographic equipment; Y. Marchuk for blastocyst injection; M. Lawrance for histology; J. Simon and E. Grabowski for artwork; and E. Stevens for administrative assistance. Y. B. was supported by a long-term EMBO fellowship and by funds from the Charles and Anna Stern Foundation. Work at the National Center for Microscopy and Imaging Research at the University of California, San Diego was supported by NIH grant #RR04050 to Dr. M. H. Ellisman. R. M. E. is an investigator of the Howard Hughes Medical Institute at the Salk Institute and March of Dimes chair in molecular and developmental biology. This work was supported in part by NIH grant #HD27183 to R. M. E.

Received June 2, 1999; revised August 17, 1999.

References

Barak, Y., Gottlieb, E., Juven-Gershon, T., and Oren, M. (1994). Regulation of mdm2 expression by p53: alternative promoters produce transcripts with nonidentical translation potential. Genes Dev. *8*, 1739–1749.

Braissant, O., and Wahli, W. (1998). Differential expression of peroxisome proliferator-activated receptor-α, -β, and -γ during rat embryonic development. Endocrinology *139*, 2748–2754.

Chen, J,. Kubalak, S.W., and Chien, K.R. (1998). Ventricular muscle-restricted targeting of the RXRα gene reveals a non-cell-autonomous requirement in cardiac chamber morphogenesis. Development *125*, 1943–1949.

Chien, K.R. (1993). Molecular advances in cardiovascular biology. Science *260*, 916–917.

Copp, A.J. (1995). Death before birth: clues from gene knockouts and mutations. Trends Genet. *11*, 87–93.

Enders, A.C. (1965). A comparative study of the fine structure of the trophoblast in several hemochorial placentas. Am. J. Anat. *116*, 29–68.

Forman, B.M., Tontonoz, P., Chen, J., and Evans, R.M. (1995). 15-Deoxy-$\Delta^{12,14}$-prostaglandin J2 is a ligand for the adipocyte determination factor PPARγ. Cell *83*, 803–812.

Forman, B.M., Chen, J., and Evans, R.M. (1997). Hypolipidemic drugs, polyunsaturated fatty acids, and eicosanoids are ligands for peroxisome-activated receptors α and δ. Proc. Natl. Acad. Sci. USA *94*, 4312–4317.

Friedman, W.F. (1988). Congenital heart disease in infancy and childhood; acquired heart disease in infancy and childhood. In Heart Disease: A Textbook of Cardiovascular Medicine, Third Edition, E. Braundwald, ed. (Philadelphia: W.B. Saunders), pp. 895–918.

Hogan, B., Beddington, R., Constantini, F., and Lacy, E. (1994). Manipulating the Mouse Embryo (New York: Cold Spring Harbor Laboratory Press), pp. 373–375.

Isseman, I., and Green, S. (1990). Activation of a member of the steroid hormone receptor superfamily by peroxisome proliferators. Nature *347*, 645–650.

Jain, S., Pulikuri, S., Zhu, Y., Qi, C., Kanwar, Y.S., Yeldandi, A.V., Rao, M.S., and Reddy, J.K. (1998). Differential expression of the peroxisome proliferator-activated receptor γ (PPARγ) and its coactivators steroid receptor coactivator-1 and PPAR-binding protein PBP in the brown fat, urinary bladder, colon, and breast of the mouse. Am. J. Pathol. *153*, 349–354.

Jollie, W.P. (1964). Fine structural changes in placental labyrinth of the rat with increasing gestational age. J. Ultrastruct. Res. *10*, 27–47.

Kastner, P., Grondona, J.M., Mark, M., Gansmuller, A., Lemeur, M., Decimo, D., Vonesch, J.L., Dolle, P., and Chambon, P. (1994). Genetic analysis of RXRα developmental function: convergence of RXR and RAR signaling pathways in heart and eye morphogenesis. Cell *78*, 987–1003.

Kastner, P., Mark, M., and Chambon, P. (1995). Nonsteroid nuclear receptors: what are genetic studies telling us about their role in real life? Cell *83*, 859–869.

Kastner, P., Messaddeq, N., Mark, M., Wendling, O., Grondona, J.M., Ward, S., Ghyselinck, N., and Chambon, P. (1997). Vitamin A deficiency and mutations of RXRα, RXRβ and RARα lead to early differentiation of embryonic ventricular cardiomyocytes. Development *124*, 4749–4758.

Kliewer, S.A., Umesono, K., Mangelsdorf, D.J., and Evans, R.M. (1992a). Retinoid X receptor interacts with nuclear receptors in retinoic acid, thyroid hormone, and vitamin D_3 signaling. Nature *355*, 446–449.

Kliewer, S.A., Umesono, K., Noonan D.J., Heyman, R.A., and Evans, R.M. (1992b). Convergence of 9-cis retinoic acid and peroxisome proliferator signaling pathways through heterodimer formation of their receptors. Nature *358*, 771–774.

Kliewer, S.A., Forman, B.M., Blumberg, B., Ong, E.S., Borgmeyer, U., Mangelsdorf, D.J., Umesono, K., and Evans, R.M. (1994). Differential expression and activation of a family of murine peroxisome proliferator-activated receptors. Proc. Natl. Acad. Sci. USA *91*, 7355–7359.

Kliewer, S.A., Lenhard, J.M., Wilson, T.M., Patel, I., Morris, D.C., and Lehmann, J.M. (1995). A prostaglandin J2 metabolite binds peroxisome proliferator-activated receptor γ and promotes adipocyte differentiation. Cell *83*, 813–819.

Lee, S.S.-T., Pineau, T., Drago, J., Lee, E.J., Owens, J.W., Kroetz, D.L., Fernandez-Salguero, P.M., Westphal, H., and Gonzalez, F.J. (1995). Targeted disruption of the α isoform of the peroxisome proliferator-activated receptor gene in mice results in abolishment of the pleiotropic effects of peroxisome proliferators. Mol. Cell. Biol. *15*, 3012–3022.

Lehmann, J.M., Moore, L.B., Smith-Oliver, T.A., Wilkison, W.O., Wilson, T.M., and Kliewer, S.A. (1995). An antidiabetic thiazolidinedione is a high affinity ligand for peroxisome proliferator-activated receptor γ (PPARγ). J. Biol. Chem. *270*, 12953–12956.

Mangelsdorf, D.J., Thummel, C., Beato, M., Herrlich, P., Schutz, G., Umesono, K., Blumberg, B., Kastner, P., Mark, M., Chambon, P., and Evans, R.M. (1995). The nuclear receptor superfamily: the second decade. Cell *83*, 835–839.

Moitra, J., Mason, M.M., Olive, M., Krylov, D., Gavrilova, O., Marcus-Samuels, B., Feigenbaum, L., Lee, E., Aoyama, T., Eckhaus, M., Reitman, M.L., and Vinson, C. (1998). Life without white fat: a transgenic mouse. Genes Dev. *12*, 3168–3181.

Mukherjee, R., Davies, P.J.A., Crombie, D.L., Bischoff, E.D., Cesario, R.M., Jow, L., Hamann, L.G., Boehm, M.F., Mondon, C.E., Nadzan, A.M., et al. (1997). Sensitization of diabetic and obese mice to insulin by retinoid X receptor agonists. Nature *386*, 407–410.

Nagy, A., and Rossant, J. (1993). Production of completely ES cell-derived fetuses. In Gene Targeting: A Practical Approach, A. Joyner, ed. (Oxford: IRL Press at Oxford University Press), pp. 147–179.

Nagy, A., Gocza, E., Merentes Diaz, E., Prideaux, V.R., Ivanyi, E., Markkula, M., and Rossant, J. (1990). Embryonic stem cels alone are able to support fetal development in the mouse. Development *110*, 815–821.

Nagy, L., Tontonoz, P., Alvarez, J.G., Chen, H., and Evans, R.M. (1998). Oxidized LDL regulates macrophage gene expression through ligand activation of PPARγ. Cell *93*, 229–240.

Olson, E.N., and Srivastava, D. (1996). Molecular pathways controlling heart development. Science *272*, 671–676.

Rossant, J. (1996). Mouse mutants and cardiac development: new molecular insights into cardiogenesis. Circ. Res. *78*, 349–353.

Ruiz-Lozano, P., Smith, S.M., Perkins, G., Kubalak, S.W., Boss, G.R., Sucov, H.M., Evans, R.M., and Chien, K.R. (1998). Energy deprivation and a deficiency in downstream metabolic target genes during the onset of embryonic heart failure in RXRα$^{-/-}$ embryos. Development *125*, 533–544.

Saez, E., Tontonoz, P., Nelson, M.C., Alvarez, J.G.A., U, T.-M., Baird, S.M., Thomazy, V.A., and Evans, R.M. (1998). Activators of the nuclear receptor PPARγ enhance colon polyp formation. Nat. Med. *4*, 1058–1061.

Sapin, V., Ward, S.J., Bronner, S., Chambon, P., and Dolle, P. (1997a). Differential expression of transcripts encoding retinoid binding proteins and retinoic acid receptors during placentation of the mouse. Dev. Dyn. *208*, 199–210.

Sapin, V., Dolle, P., Hindelang, C., Kastner, P., and Chambon, P. (1997b). Defects of the chorioallantoic placenta in mouse RXRα null fetuses. Dev. Biol. *191*, 29–41.

Schaeren-Wiemars, M., and Gerfin-Moser, A. (1993). A single protocol to detect transcripts of various types and expression levels in neural tissue and cultured cells: in situ hybridization using digoxygenin-labeled cRNA probes. Histochemistry *100*, 431–440.

Schoonjans, K., Peinado-Onsurbe, J., Lefebvre, A.-M., Heyman, R.A., Briggs, M., Deeb, S., Staels, B., and Auwerx, J. (1996). PPARα and PPARγ activators direct a distinct tissue-specific transcriptional response via a PPRE in the lipoprotein lipase gene. EMBO J. *15*, 5336–5348.

Sears, I.B., MacGinnitie, M.A., Kovacs, L.G., and Graves, R.A. (1996). Differentiation-dependent expression of the brown adipocyte uncoupling protein gene: regulation by peroxisome proliferator activated receptor γ. Mol. Cell. Biol. *16*, 3410–3418.

Seip, M., and Trygstad, O. (1996). Generalized lipodystrophy, congenital and acquired (lipoatrophy). Acta Paediatr. Scand. Suppl. *413*, 2–28.

Sengers, R.C., Stadhouders, A.M., and Trijbels, J.M. (1984). Mitochondrial myopathies: clinical, morphological and biochemical aspects. Eur. J. Pediatr. *141*, 192–207.

Shimomura, I., Hammer, R.E., Richardson, J.A., Ikemoto, S., Bashmakov, Y., Goldstein, J.L., and Brown, M.S. (1998). Insulin resistance and diabetes mellitus in transgenic mice expressing nuclear SREBP-1c adipose tissue: model for congenital generalized lipodystrophy. Genes Dev. *12*, 3182–3194.

Spiegelman, B.M., and Flier, J.S. (1996). Adipogenesis and obesity: rounding out the big picture. Cell *87*, 377–389.

Sucov, H.M., Dyson, E., Gumeringer, C., Price, J., Chien, K.R., and Evans, R.M. (1994). RXRα mutant mice establish a genetic basis for vitamin A signaling in heart morphogenesis. Genes Dev. *8*, 1007–1018.

Tontonoz, P., Hu, E., and Spiegelman, B.M. (1994a). Stimulation of adipogenesis in fibroblasts by PPARγ2, a lipid-activated transcription factor. Cell *79*, 1147–1156.

Tontonoz, P., Hu, E., Graves, R.A., Budavari, A.I., and Spiegelman, B.M. (1994b). mPPARγ2: tissue-specific regulator of an adipocyte enhancer. Genes Dev. *8*, 1224–1234.

Tontonoz, P., Singer, S., Forman, B.M., Sarraf, P., Fletcher, J.A., Fletcher, C.D.M., Brun, R.P., Mueller, E., Altiok, S., Oppenheim, H., et al. (1997). Terminal differentiation of human liposarcoma cells induced by ligands for peroxisome proliferator-activated receptor γ and the retinoid X receptor. Proc. Natl. Acad. Sci. USA *94*, 237–241.

Tontonoz, P., Nagy, L., Alvarez, J.G., Thomazy, V.A., and Evans, R.M. (1998). PPARγ promotes monocyte/macrophage differentiation and uptake of oxidized LDL. Cell *93*, 241–252.

Tran, C.M., and Sucov, H.M. (1998). The RXRα gene functions in a non-cell-autonomous manner during mouse cardiac morphogenesis. Development *125*, 1951–1956.

Wendling, O., Chambon, P., and Mark, M. (1999). Retinoid X receptors are essential for early mouse development and placentogenesis. Proc. Natl. Acad. Sci. USA *96*, 547–551.